

QRAP: a numerical code for projected (Q)uasi-particle (RA)ndom (P)hase approximation

F. Krmpotić¹, A. R. Samana² and C. A. Bertulani^{2*}

¹*Departamento de Física and Facultad de Ciencias Astronómicas y Geofísicas, Universidad Nacional de La Plata, C. C. 67, 1900 La Plata, Argentina and*

²*Department of Physics, Texas A&M University Commerce, P.O.3011 Commerce, 75429 TX, USA*
(Dated: June 23, 2009)

Abstract

A computer code for quasiparticle random phase approximation-QRPA and projected quasiparticle random phase approximation-PQRPA models of nuclear structure is explained in details. An important application of the code consists in evaluating nuclear matrix elements involved in neutrino-nucleus reactions. As an example, cross section for ^{56}Fe and ^{12}C are calculated and the code output is explained. The application to other nuclei and the description of other nuclear and weak decay processes is also discussed.

Program summary

Title of program: QRAP (Quasiparticle RAndom Phase approximation)

Computers: The code has been created on an PC, but also runs on UNIX or LINUX machines.

Operating systems: WINDOWS or UNIX

Program language used: Fortran-77

Memory required to execute with typical data: 16 Mbytes of RAM memory and 2 MB of hard disk space

No. of lines in distributed program, including test data, etc.: $\sim 8,000$

No. of bytes in distributed program, including test data, etc.: $\sim 256\text{ kB}$

Distribution format: tar.gz

Keywords: QRPA; Projected QRPA; semileptonic processes.

Nature of physical problem: The program calculates neutrino- and antineutrino-nucleus cross sections as a function of the incident neutrino energy, and muon capture rates, using the QRPA or PQRPA as nuclear structure models.

Method of solution: The QRPA, or PQRPA, equations are solved in a self-consistent way for even-even nuclei. The nuclear matrix elements for the neutrino-nucleus interaction are treated as the beta inverse reaction of odd-odd nuclei as function of the transfer momentum.

Typical running time: $\approx 5\text{ min}$ on a 3 GHz processor for Data set 1.

PACS numbers: 21.60.Jz, 25.30.Pt, 26.30.Jk

Long Write-Up

I. INTRODUCTION

The new age of the physics beyond the standard model of electroweak interaction has as one of the most promising pathways the search of neutrino oscillations. Several experimental efforts are oriented to find the neutrino masses and the related oscillations involving atmospheric, solar, reactor and accelerator neutrinos [1, 2, 3, 4, 5]. Since neutrinos interact so weakly with matter, they bring information on the dynamics of supernova collapse and posterior explosion as well as on the synthesis of heavy nuclei [6, 7].

The detection signal of neutrinos is measured through the weak interaction of incoming neutrinos with the nu-

clei present in, e.g., a liquid scintillator detector, as well as with the surrounding blockhouse detector-shield. The flux-averaged ν -nucleus cross sections are the measured observables. Recently, Ref. [8] has studied the effect of neutrino oscillations on the expected supernova neutrino signal with the LVD detector, through their interactions with protons and carbon nuclei in a liquid scintillator and with iron nuclei in the support structure.

Charged and neutral ν_e -nucleus cross sections on ^{12}C (liquid scintillator) as well as on ^{56}Fe (detector surrounding shield) were measured by the KARMEN Collaboration [9, 10]. Other experiments such as LAMPF [11, 12] and LSND [13, 14] have also used ^{12}C to search for neutrino oscillations and to measure neutrino-nucleus cross sections. Furthermore, future experiments will use ^{12}C as liquid scintillator, such as in the spallation neutron source (SNS) at Oak Ridge National Laboratory (ORNL) [15], or in the LVD (Large Volume Detector) experiment [8].

On the other hand, the cross sections $\nu_e(\bar{\nu}_e)-^{56}\text{Fe}$ are important to test the ability of nuclear models in explaining reactions on nuclei with masses around iron, which

*Electronic address: krmpotic@venus.fisica.unlp.edu, arturo.samana@tamuc.edu

play an important role in supernova collapse [16]. The iron is used as material detector in experiments on neutrino oscillations such as MINOS [17], whereas future experiments, such as SNS at ORNL [15] plan to use the same material.

There have been intensive efforts on nuclear structure models to describe consistently semileptonic weak processes with ^{12}C such as RPA-like models. A brief summary on the different models employed for ^{12}C is sketched in Ref. [18].

The QRAP code is based on the works presented in Refs.[19, 20, 21]. The code was written to solve numerically a known puzzle in Random Phase Approximation (RPA)-models when applied to the weak observables in the triad $\{^{12}\text{B}, ^{12}\text{C}, ^{12}\text{N}\}$. The code uses the Projected Quasi-Particle RPA, or PQRPA, model as a theoretical framework. The employment of PQRPA for the inclusive $^{12}\text{C}(\nu_e, e^-)^{12}\text{N}$ cross section, instead of the continuum RPA (CRPA) used by the LSND collaboration in the analysis of $\nu_\mu \rightarrow \nu_e$ oscillations of the 1993-1995 data sample, leads to an increased oscillation probability [22]. The projection procedure employed in Ref. [19] was essential to solve the problem in determining the ground state of ^{12}N when the QRPA of Ref. [23] was not properly accounting for configuration mixing. The nuclear structure programming for the QRPA model with the residual δ -interaction has been used extensively in the literature [24, 25, 26, 27, 28] to describe the single and double beta decays. Moreover, the PQRPA derived from the time-dependent variational principle was used to study the two-neutrino $\beta\beta$ -decay in ^{76}Ge [29]. In that work, the projection procedure was less important and the QRPA and PQRPA yield qualitatively similar results.

The PQRPA was recently used to calculate the $^{56}\text{Fe}(\nu_e, e^-)^{56}\text{Co}$ cross section [20]. A comparison of QRPA and PQRPA with the same interaction and in the same space model show us that the projection procedure is important for medium mass nuclei. Moreover, several approximations such as the Hybrid model (shell model for allowed and RPA for forbidden transitions) [30], QRPA with Skyrme interaction [31], Relativistic QRPA [32], and QRPA and PQRPA [20] yield differences of the neutrino cross section as a function of the neutrino energy. It is a hard task to find the origin for the differences, mainly because these models are not using the same interaction and/or the same single-particle configuration space, carrying different types of correlations in each case. Ref. [33] has been able to constrain theoretical shell models for inelastic neutrino-induced cross sections on nuclei, which are proportional to the $B(GT_0)$ at low neutrinos energies, with medium-mass nuclei present in supernova environment using experimental data on the M1 magnetic dipole strength. Nevertheless, there is no similar study with charged neutrino-induced cross sections, although the calculations performed in Ref. [34] using the hybrid model are in the correct ballpark. The main difficulty presented by the shell model in this work is the great computational effort to describe the momentum-transfer

dependence of the Gamow-Teller operator. Therefore, the authors scale the shell model Gamow-Teller cross sections using the ratios obtained by RPA calculations with and without q -dependence of the multipole operator.

This brief introduction shows the importance of (i) to calculate neutrino-nucleus cross sections for astrophysical purposes and, (ii) that these cross sections are strongly correlated with the nuclear structure model employed. The QRAP code, with a simple residual interaction, is able to access the sources of these problems and it can calculate several weak interaction processes mentioned above.

This write-up is organized as follows. In section II we make a short survey of the theoretical description of weak interaction processes, with emphasis on the formulation implemented in this numerical code. In sections III and IV we describe the RPA, QRPA, and PQRPA formalisms, making explicit the differences among them. In section V we show how the code is organized, how to make an input and how to understand the output. Section VI explains the role of each subroutine of the code. Finally, section VII proposes a few cases to practice with the code.

II. WEAK INTERACTING PROCESSES

It was shown in Ref. [21] that several existing formalisms in the literature for neutrino-nucleus interactions are equivalent. The weak interacting processes can be described by: 1) seven nuclear matrix elements (NME), when they explicitly dependent on both the orbital momentum (L) and the total angular momentum (J), being four of them non-relativistic (NRNME) and two relativistic (RNME) [35, 36], or 2) by only two NRNME and two RNME, when only J is considered to be a good quantum number [21]. There is also an hybrid formalism [37] with three NRNME.

In this section we give a brief summary of the main formulae developed in Ref. [21] for

- neutrino scattering (NS)

$$\nu_\ell + (Z, A) \rightarrow (Z + 1, A) + \ell^-,$$

- antineutrino scattering (AS)

$$\bar{\nu}_\ell + (Z, A) \rightarrow (Z - 1, A) + \ell^+,$$

- muon capture (MC) rate

$$\mu^- + (Z, A) \rightarrow (Z - 1, A) + \nu_\mu,$$

where $\ell = e, \mu$.

The weak Hamiltonian is expressed in the form [35, 36, 38]

$$H_w(\mathbf{r}) = \frac{G}{\sqrt{2}} J_\alpha l_\alpha e^{-i\mathbf{r}\cdot\mathbf{k}}, \quad (2.1)$$

where $G = (3.04545 \pm 0.00006) \times 10^{-12}$ is the Fermi coupling constant (in natural units),

$$J_\alpha \equiv (\mathbf{J}, iJ_\emptyset) \quad (2.2)$$

$$= i\gamma_4 \left[g_V \gamma_\alpha - \frac{g_M}{2M} \sigma_{\alpha\beta} k_\beta + g_A \gamma_\alpha \gamma_5 + i \frac{g_P}{m_\ell} k_\alpha \gamma_5 \right],$$

is the hadronic current operator¹, and

$$l_\alpha(\mathbf{q}, E_\nu) \equiv (\mathbf{l}, il_\emptyset) = -i\bar{u}_{s_\ell}(\mathbf{p}, E_\ell) \gamma_\alpha (1 + \gamma_5) u_{s_\nu}, \quad (2.3)$$

is the plane wave approximation for the matrix element of the leptonic current in the case of neutrino reactions, with $p_\ell \equiv \{\mathbf{p}, iE_\ell\}$ and $q_\nu \equiv \{\mathbf{q}, iE_\nu\}$ being, respectively, the lepton and the neutrino momenta.

For the sake of convenience we will use spherical coordinates ($M = -1, 0, +1$) for the three-vectors, and the Walecka's notation [36], with the Euclidean metric, for four-vectors, *i.e.*, $x = \{\mathbf{x}, x_4 = ix_0\}$. The only difference is that we substitute Walecka's indices (0, 3) by our indices ($\emptyset, 0$), *i.e.* we use the index \emptyset for the temporal component and the index 0 for the third spherical component.

The quantity

$$k = P_i - P_f \equiv \{\mathbf{k}, ik_\emptyset\}, \quad (2.4)$$

is the momentum transfer, where P_i and P_f are momenta of the initial and final nucleus, M is the nucleon mass, m_ℓ is the mass of the charged lepton, and g_V, g_A, g_M and g_P are, respectively, the vector, axial-vector, weak-magnetism and pseudoscalar effective dimensionless coupling constants. Their numerical values are:

$$g_V = 1; g_A = 1.26;$$

$$g_M = \kappa_p - \kappa_n = 3.70; g_P = g_A \frac{2Mm_\ell}{k^2 + m_\pi^2}. \quad (2.5)$$

In the numerical calculations we use an effective axial-vector coupling $g_A = 1$ [39].

The finite nuclear size (FNS) effect is incorporated via the dipole form factor with a cutoff $\Lambda = 850$ MeV, *i.e.*,

$$g \rightarrow g \left(\frac{\Lambda^2}{\Lambda^2 + k^2} \right)^2. \quad (2.6)$$

To use (2.1) with the non-relativistic nuclear wave functions, the Foldy-Wouthuysen transformation has to be performed on the hadronic current (2.2). When the velocity dependent terms are included this yields:

$$J_\emptyset = g_V + (\bar{g}_A + \bar{g}_{P1}) \boldsymbol{\sigma} \cdot \hat{\mathbf{k}} - g_A \boldsymbol{\sigma} \cdot \mathbf{v},$$

$$\mathbf{J} = -g_A \boldsymbol{\sigma} - i\bar{g}_W \boldsymbol{\sigma} \times \hat{\mathbf{k}} - \bar{g}_V \hat{\mathbf{k}} + \bar{g}_{P2} (\boldsymbol{\sigma} \cdot \hat{\mathbf{k}}) \hat{\mathbf{k}} + g_V \mathbf{v}, \quad (2.7)$$

where $\hat{\mathbf{k}} = \mathbf{k}/\kappa$, $\kappa \equiv |\mathbf{k}|$, and $\mathbf{v} \equiv -i\nabla/M$ is the velocity operator, acting on the nuclear wave functions. The following short notation

$$\bar{g}_V = g_V \frac{\kappa}{2M}; \bar{g}_A = g_A \frac{\kappa}{2M}; \bar{g}_W = (g_V + g_M) \frac{\kappa}{2M},$$

$$\bar{g}_{P1} = g_P \frac{\kappa}{2M} \frac{q_0}{m_\ell}; \bar{g}_{P2} = g_P \frac{\kappa}{2M} \frac{\kappa}{m_\ell}, \quad (2.8)$$

has also been introduced.

In performing the multipole expansion of the nuclear operators

$$O_\alpha \equiv (\mathbf{O}, O_\emptyset) = J_\alpha e^{-i\mathbf{k} \cdot \mathbf{r}}, \quad (2.9)$$

it is convenient

1) to take the momentum \mathbf{k} to be along the z axis, *i.e.*,

$$e^{-i\mathbf{k} \cdot \mathbf{r}} = \sum_L i^{-L} \sqrt{4\pi(2L+1)} j_L(\rho) Y_{L0}(\hat{\mathbf{r}}),$$

$$= \sum_J i^{-J} \sqrt{4\pi(2J+1)} j_J(\rho) Y_{J0}(\hat{\mathbf{r}}), \quad (2.10)$$

where $\rho = \kappa r$, and

2) to define the operators O_α as

$$O_\alpha \equiv (\mathbf{O}, O_\emptyset) = \sqrt{4\pi} \sum_J i^{-J} \sqrt{2J+1} O_{\alpha J}. \quad (2.11)$$

Thus,

$$O_{\emptyset J} = j_J(\rho) Y_{J0}(\hat{\mathbf{r}}) J_\emptyset,$$

$$O_{MJ} = \sum_L i^{J-L} F_{MLJ} j_L(\rho) [Y_L(\hat{\mathbf{r}}) \otimes \mathbf{J}]_{JM}, \quad (2.12)$$

where the geometrical factors

$$F_{MJL} \equiv (-)^{J+M} \sqrt{(2L+1)} \begin{pmatrix} L & 1 & J \\ 0 & -M & M \end{pmatrix}, \quad (2.13)$$

are listed in Table I of Ref. [21].

Explicitly, from (2.7)

$$O_{\emptyset J} = g_V \mathcal{M}_J^V + 2i\bar{g}_A \mathcal{M}_J^A + i(\bar{g}_A + \bar{g}_{P1}) \mathcal{M}_{0J}^A, \quad (2.14)$$

$$O_{MJ} = i(\delta_{M0} \bar{g}_{P2} - g_A + M\bar{g}_W) \mathcal{M}_{MJ}^A$$

$$+ 2\bar{g}_V \mathcal{M}_{MJ}^V - \delta_{M0} \bar{g}_V \mathcal{M}_J^V. \quad (2.15)$$

The elementary operators are given by

$$\mathcal{M}_J^V = j_J(\rho) Y_J(\hat{\mathbf{r}}),$$

$$\mathcal{M}_J^A = \kappa^{-1} j_J(\rho) Y_J(\hat{\mathbf{r}}) (\boldsymbol{\sigma} \cdot \nabla),$$

$$\mathcal{M}_{MJ}^A = \sum_L i^{J-L-1} F_{MLJ} j_L(\rho) [Y_L(\hat{\mathbf{r}}) \otimes \boldsymbol{\sigma}]_J, \quad (2.16)$$

$$\mathcal{M}_{MJ}^V = \kappa^{-1} \sum_L i^{J-L-1} F_{MLJ} j_L(\rho) [Y_L(\hat{\mathbf{r}}) \otimes \nabla]_J.$$

¹ To avoid confusion, we will be using roman fonts (M, m) for masses and math italic fonts (M, m) for azimuthal quantum numbers.

Here we make use of the conserved vector current (CVC). From (2.14), (2.15), and [40, Eq. (10.45) and (9.7)]

$$\mathbf{k} \cdot \mathbf{O}^V = \kappa O_0^V = k_\theta O_\theta^V \quad (2.17)$$

which yields

$$2\bar{g}_V \mathcal{M}_{0J}^V - \bar{g}_V \mathcal{M}_J^V = \frac{k_\theta}{\kappa} g_V \mathcal{M}_J^V. \quad (2.18)$$

Thus, from (2.15)

$$\begin{aligned} \mathbf{O}_{MJ} &= i(\delta_{M0} \bar{g}_{P2} - g_A + M \bar{g}_W) \mathcal{M}_{MJ}^A \\ &+ 2|M| \bar{g}_V \mathcal{M}_{MJ}^V + \delta_{M0} \frac{k_\theta}{\kappa} g_V \mathcal{M}_J^V. \end{aligned} \quad (2.19)$$

The elementary operators \mathcal{M}_J^V , \mathcal{M}_J^A , \mathcal{M}_{0J}^A and \mathcal{M}_{0J}^V are real, but $\mathcal{M}_{\pm 1J}^A$ and $\mathcal{M}_{\pm 1J}^V$ are not, and it is convenient to put in evidence their real and imaginary parts, expressing them as

$$\mathcal{M}_{\pm 1J} = \tilde{\mathcal{M}}_{1J} \pm i \hat{\mathcal{M}}_{1J} \quad (2.20)$$

with $\tilde{\mathcal{M}}_{1J}$, and $\hat{\mathcal{M}}_{1J}$ arising, respectively, from the terms in (2.16) with $L = J \pm 1$, and $L = J$. Note that $F_{\pm 1JJ} = \mp 1/\sqrt{2}$.

It is also convenient to separate the elementary operators into:

- *natural parity* (NP), ($\pi = (-)^J$): \mathcal{M}_J^V , $\hat{\mathcal{M}}_{1J}^A$, and $\tilde{\mathcal{M}}_{1J}^V$, and
- *unnatural parity* (UP), ($\pi = (-)^{J+1}$): \mathcal{M}_J^A , $\hat{\mathcal{M}}_{1J}^V$, \mathcal{M}_{0J}^A , and $\tilde{\mathcal{M}}_{1J}^A$

The operators $\mathbf{O}_{\alpha J} \equiv (\mathbf{O}_{0J}, \mathbf{O}_{MJ})$ can be cast as a sum of real and imaginary operators, *i.e.*, $\mathbf{O}_{\alpha J} = \mathbf{O}_{\alpha J}^{\Re} + i \mathbf{O}_{\alpha J}^{\Im}$, with $\mathbf{O}_{\alpha J}^{\Re}$ ($\mathbf{O}_{\alpha J}^{\Im}$) being a NP (UP) operator. This is a very important finding because it implies that $\mathbf{O}_{\alpha J}^{\Re}$ and $\mathbf{O}_{\alpha J}^{\Im}$ *do not contribute simultaneously*, and, therefore, *one always can deal only with real operators*.

In summary, natural and unnatural parity operators are, respectively:

$$\begin{aligned} \mathbf{O}_{0J}^{\Re} &= g_V \mathcal{M}_J^V, \\ \mathbf{O}_{0J}^{\Im} &= \frac{k_\theta}{\kappa} g_V \mathcal{M}_J^V, \\ \mathbf{O}_{M \neq 0J}^{\Re} &= (M g_A - \bar{g}_W) \hat{\mathcal{M}}_{1J}^A + 2\bar{g}_V \tilde{\mathcal{M}}_{1J}^V, \end{aligned} \quad (2.21)$$

and

$$\begin{aligned} \mathbf{O}_{0J}^{\Im} &= 2\bar{g}_A \mathcal{M}_J^A + (\bar{g}_A + \bar{g}_{P1}) \mathcal{M}_{0J}^A, \\ \mathbf{O}_{0J}^{\Re} &= (\bar{g}_{P2} - g_A) \mathcal{M}_{0J}^A, \\ \mathbf{O}_{M \neq 0J}^{\Im} &= (-g_A + M \bar{g}_W) \hat{\mathcal{M}}_{1J}^A + 2M \bar{g}_V \hat{\mathcal{M}}_{1J}^V. \end{aligned} \quad (2.22)$$

A. Neutrino-nucleus cross section

For the neutrino-nucleus reaction, the momentum transfer is $k = p_\ell - q_\nu$, and the corresponding cross section reads

$$\sigma(E_\ell, J_f) = \frac{|\mathbf{p}_\ell| E_\ell}{2\pi} F(Z \pm 1, E_\ell) \int_{-1}^1 d(\cos \theta) \mathcal{T}_\sigma(\mathbf{q}, J_f), \quad (2.23)$$

where $F(Z \pm 1, E_\ell)$ is the Fermi function ($Z + 1$, for neutrino, and $Z - 1$, for antineutrino), $\theta \equiv \hat{\mathbf{q}} \cdot \hat{\mathbf{p}}$ is the angle between the incident neutrino and ejected lepton, and the transition amplitude is

$$\mathcal{T}_\sigma(\kappa, J_f) = \frac{1}{2J_i + 1} \sum_{s_\ell, s_\nu} \sum_{M_i, M_f} |\langle J_f M_f | H_W | J_i M_i \rangle|^2. \quad (2.24)$$

After expressing the spatial part of the lepton traces $\mathcal{L}_{\alpha\beta}$ in spherical coordinates, and applying the Wigner-Eckart theorem, one can cast the transition amplitude in the compact form [21]

$$\begin{aligned} \mathcal{T}_\sigma(\kappa, J_f) &= \frac{4\pi G^2}{2J_i + 1} \sum_J [|\langle J_f || \mathbf{O}_{0J} || J_i \rangle|^2 \mathcal{L}_\theta \\ &+ \sum_{M=0\pm 1} |\langle J_f || \mathbf{O}_{MJ} || J_i \rangle|^2 \mathcal{L}_M \\ &- 2\Re(\langle J_f || \mathbf{O}_{0J} || J_i \rangle \langle J_f || \mathbf{O}_{0J} || J_i \rangle) \mathcal{L}_{\theta 0}]. \end{aligned} \quad (2.25)$$

The explicit expressions for the traces $\mathcal{L}_\theta \equiv \mathcal{L}_{\theta\theta}$, $\mathcal{L}_M \equiv \mathcal{L}_{MM}$, and $\mathcal{L}_{\theta 0}$ are [21]

$$\begin{aligned} \mathcal{L}_{\theta\theta} &= 1 + \frac{|\mathbf{p}| \cos \theta}{E_\ell}, \\ \mathcal{L}_{\theta 0} &= \left(\frac{q_0}{E_\nu} + \frac{p_0}{E_\ell} \right), \\ \mathcal{L}_0 &= 1 + \frac{2q_0 p_0}{E_\ell E_\nu} - \frac{|\mathbf{p}| \cos \theta}{E_\ell}, \\ \mathcal{L}_{\pm 1} &= 1 - \frac{q_0 p_0}{E_\ell E_\nu} \pm \left(\frac{q_0}{E_\nu} - \frac{p_0}{E_\ell} \right) S_1, \end{aligned} \quad (2.26)$$

with

$$\begin{aligned} q_0 &= \hat{k} \cdot \mathbf{q} = \frac{E_\nu (|\mathbf{p}| \cos \theta - E_\nu)}{\kappa}, \\ p_0 &= \hat{k} \cdot \mathbf{p} = \frac{|\mathbf{p}| (|\mathbf{p}| - E_\nu \cos \theta)}{\kappa}, \end{aligned} \quad (2.27)$$

being the z -components of the neutrino and lepton momenta, and $S_1 = \pm 1$ for NS and AS, respectively.

B. μ -capture rates

The muon capture transition amplitude $\mathcal{T}_{MC}(J_f)$ can be derived from the result (2.25) for the neutrino-nucleus

reaction amplitude, by keeping in mind that: i) the roles of p and q are interchanged within the matrix elements of the leptonic current, which makes that in (2.26) $S_1 \rightarrow -1$, ii) the momentum transfer turns out to be $k = q - p$, and therefore the signs on the right-hand sides of (q_0, p_0) have to be changed, and iii) the threshold values ($\mathbf{p} \rightarrow 0 : \mathbf{q} \rightarrow \mathbf{k}, k_0 \rightarrow E_\nu - m_\ell$) must be used for the lepton traces. All this yields $q_0 = E_\nu, p_0 = 0$, and

$$\mathcal{L}_{\emptyset\emptyset} = \mathcal{L}_{\emptyset 0} = \mathcal{L}_0 = 1, \quad \mathcal{L}_1 = 0, \quad \mathcal{L}_{-1} = 2. \quad (2.28)$$

Instead of summing over the initial lepton spins s_ℓ , as done in (2.24), one has now to average over the same quantum number. We get

$$\Lambda(J_f) = \frac{E_\nu^2}{2\pi} |\phi_{1S}|^2 \mathcal{T}_{MC}(J_f), \quad (2.29)$$

where ϕ_{1S} is the muonic bound state wave function evaluated at the origin, and $E_\nu = m_\mu - (M_n - M_p) - E_B^\mu - E_f + E_i$, where E_B^μ is the binding energy of the muon in the $1S$ orbit. Thus from (2.25) and (2.28)

$$\begin{aligned} \mathcal{T}_\sigma(\kappa, J_f) &= \frac{4\pi G^2}{2J_i + 1} \sum_J [|\langle J_f || \mathcal{O}_{0J} - \mathcal{O}_{0J} || J_i \rangle|^2 \\ &+ 2|\langle J_f || \mathcal{O}_{-1J} || J_i \rangle|^2]. \end{aligned} \quad (2.30)$$

In the case of MC it is convenient to rewrite the effective coupling constants (2.8) as

$$\begin{aligned} \bar{g}_v &= g_v \frac{E_\nu}{2M}; \quad \bar{g}_A = g_A \frac{E_\nu}{2M}; \\ \bar{g}_w &= (g_v + g_M) \frac{E_\nu}{2M}; \quad \bar{g}_p = g_p \frac{E_\nu}{2M}, \end{aligned} \quad (2.31)$$

where $\bar{g}_p = \bar{g}_{p2} - \bar{g}_{p1}$.²

Thus, natural and unnatural parity operators are now, respectively:

$$\begin{aligned} \mathcal{O}_{0J}^{\mathcal{R}} - \mathcal{O}_{0J}^{\mathcal{R}} &= (g_v - \frac{k_0}{\kappa} g_v) \mathcal{M}_J^V = g_v \frac{m_\mu}{E_\nu} \mathcal{M}_J^V, \\ \mathcal{O}_{-1J}^{\mathcal{R}} &= -(g_A + \bar{g}_w) \hat{\mathcal{M}}_{1J}^A + 2\bar{g}_v \tilde{\mathcal{M}}_{1J}^V, \end{aligned} \quad (2.32)$$

and

$$\begin{aligned} \mathcal{O}_{0J}^{\mathcal{S}} - \mathcal{O}_{0J}^{\mathcal{S}} &= 2\bar{g}_A \mathcal{M}_J^A + (g_A + \bar{g}_A - \bar{g}_p) \mathcal{M}_{0J}^A, \\ \mathcal{O}_{-1J}^{\mathcal{S}} &= -(g_A + \bar{g}_w) \hat{\mathcal{M}}_{1J}^A - 2\bar{g}_v \tilde{\mathcal{M}}_{1J}^V. \end{aligned} \quad (2.33)$$

III. NUCLEAR STRUCTURE CALCULATION

A. PQRPA

The quasiparticle random phase approximation (PQRPA) for charge-exchange excitations was derived from the time-dependent variational principle in

Ref. [29]. In the same reference is also described in details the projected Barden-Cooper-Schiffer (PBCS) approximation. In this section we give a brief description of both the PBCS and PQRPA approximations.

The PBCS gap equations are

$$2\bar{e}_k u_k v_k - \Delta_k (u_k^2 - v_k^2) = 0, \quad (3.1)$$

where

$$\Delta_k = -\frac{1}{2} \sum_{k'} \frac{(2j_{k'} + 1)^{1/2}}{(2j_k + 1)^{1/2}} u_{k'} v_{k'} G(k k k' k'; 0) \frac{I^{Z-2}(k k')}{I^Z}, \quad (3.2)$$

are the pairing gaps, and

$$\begin{aligned} \bar{e}_k &= e_k \frac{I^{Z-2}(k)}{I^Z} + \sum_{k'} \frac{(2j_{k'} + 1)^{1/2}}{(2j_k + 1)^{1/2}} v_{k'}^2 \\ &\times F(k k k' k'; 0) \frac{I^{Z-4}(k k')}{I^Z} + \Delta e_k, \end{aligned} \quad (3.3)$$

are the dressed single-particle energies, where

$$\begin{aligned} I^K(k_1 k_2 \dots k_n) &= \frac{1}{2\pi i} \oint \frac{dz}{z^{K+1}} \sigma_{k_1} \dots \sigma_{k_n} \\ &\times \prod_k (u_k^2 + z^2 v_k^2)^{j_k + 1/2}, \\ \bar{\sigma}_k^{-1} &= u_k^2 + z_k^2 v_k^2, \end{aligned} \quad (3.4)$$

are the PBCS number projection integrals. The PBCS correction term Δe_k can be found in Ref. [29], G , and F stand for the usual particle-particle (pp), and particle-hole (ph) matrix elements of the residual interaction V , *i.e.*,

$$\begin{aligned} G(p n p' n'; J) &= \langle p n; J | V | p' n'; J \rangle. \\ F(p n p' n'; J) &= \langle p n^{-1}; J | V | p' n'^{-1}; J \rangle. \end{aligned} \quad (3.5)$$

The forward-going (X_μ), and backward-going (Y_μ) PQRPA amplitudes are obtained by solving the RPA equations

$$\begin{pmatrix} A_\mu & B \\ -B^* & -A_\mu^* \end{pmatrix} \begin{pmatrix} X_\mu \\ Y_\mu \end{pmatrix} = \omega_\mu \begin{pmatrix} X_\mu \\ Y_\mu \end{pmatrix}, \quad (3.6)$$

with the PQRPA matrices defined as:

$$\begin{aligned} A_\mu(p n, p' n'; J) &= (\varepsilon_p^{Z-1+\mu} + \varepsilon_n^{N-1-\mu}) \delta_{p n, p' n'} + N_\mu^{-1/2} (p n) \\ &N_\mu^{-1/2} (p' n') \times \{ [u_p v_n u_{p'} v_{n'} I^{Z-1+\mu} (p p') I^{N-3-\mu} (n n') \\ &+ v_p u_n v_{p'} u_{n'} I^{Z-3+\mu} (p p') I^{N-1-\mu} (n n')] F(p n, p' n'; J) \\ &+ [u_p u_n u_{p'} u_{n'} I^{Z-1+\mu} (p p') I^{N-1-\mu} (n n') \\ &+ v_p v_n v_{p'} v_{n'} I^{Z-3+\mu} (p p') I^{N-3-\mu} (n n')] G(p n, p' n'; J) \}, \\ B(p n, p' n'; J) &= N_\mu^{-1/2} (p n) N_{-\mu}^{-1/2} (p' n') I^{Z-2} (p p') I^{N-2} (n n') \\ &\times [(v_p u_n u_{p'} v_{n'} + u_p v_n v_{p'} u_{n'}) F(p n, p' n'; J) \\ &+ (u_p u_n v_{p'} v_{n'} + v_p v_n u_{p'} u_{n'}) G(p n, p' n'; J)], \end{aligned} \quad (3.7)$$

² Note that there is a misprint in Eq. (2.41) of Ref. [21]. Also in Eq. (2.42) of the same reference \bar{g}_{p1} should read \bar{g}_p .

where

$$N_\mu(pn) = I^{Z-1+\mu}(p)I^{N-1-\mu}(n), \quad (3.8)$$

are the norms,

$$\varepsilon_k^K = \frac{R_0^K(k) + R_{11}^K(kk)}{I^K(k)} - \frac{R_0^K}{I^K} \quad (3.9)$$

are the projected quasiparticle energies, and the quantities R^K are defined as [29]

$$\begin{aligned} R_0^K(k) &= \sum_{k_1} (2j_{k_1} + 1)v_{k_1}^2 e_{k_1} I^{K-2}(kk_1) \\ &+ \frac{1}{4} \sum_{k_1 k_2} (2j_{k_1} + 1)^{1/2} (2j_{k_2} + 1)^{1/2} \\ &\times [v_{k_1}^2 v_{k_2}^2 F(k_1 k_1 k_2 k_2; 0) I^{K-4}(k_1 k_2 k) \\ &+ u_{k_1} v_{k_1} u_{k_2} v_{k_2} G(k_1 k_1 k_2 k_2; 0) I^{K-2}(k_1 k_2 k)], \\ R_{11}^K(kk) &= e_k [u_k^2 I^K(kk) - v_k^2 I^{K-2}(kk)] \\ &+ \sum_{k_1} \frac{(2j_{k_1} + 1)^{1/2}}{(2j_k + 1)^{1/2}} \{v_{k_1}^2 F(k_1 k_1 k k; 0) \\ &[u_k^2 I^{K-2}(k_1 k k) - v_k^2 I^{K-4}(k_1 k k)] \\ &- u_{k_1} v_{k_1} u_k v_k G(k_1 k_1 k k; 0) I^{K-2}(k_1 k k)\}. \end{aligned} \quad (3.10)$$

B. QRPA

The usual gap equations are obtained from Eqs. (3.6)-(3.7) by:

1. Making the replacement $e_k \rightarrow e_k - \lambda_k$, with λ_k being the chemical potential, and taking the limit $I^K \rightarrow 1$. That is, the Eq. (3.1) remains as it is, but instead of (3.2) and (3.3) one has now

$$\Delta_k = -\frac{1}{2} \sum_{k'} \frac{(2j_{k'} + 1)^{1/2}}{(2j_k + 1)^{1/2}} u_{k'} v_{k'} G(kk k' k'; 0), \quad (3.11)$$

and

$$\bar{e}_k = e_k - \lambda_k + \sum_{k'} \frac{(2j_{k'} + 1)^{1/2}}{(2j_k + 1)^{1/2}} v_{k'}^2 F(kk k' k'; 0). \quad (3.12)$$

2. Impose the subsidiary conditions

$$Z = \sum_{j_p} (2j_p + 1)^2 v_{j_p}^2, \quad N = \sum_{j_n} (2j_n + 1)^2 v_{j_n}^2, \quad (3.13)$$

as the number of particles is not any more a good quantum number.

In this way the usual BCS gap equations read

$$2(e_k - \lambda_t)u_k v_k = (u_k^2 - v_k^2)\Delta_k. \quad (3.14)$$

This equation coupled with the normalization condition, $u_k^2 + v_k^2 = 1$, has as solution the occupation probabilities (for example, from the Chapter I of Rowe [41], we can understand the meaning of ‘‘occupation probability’’)

$$u_k^2 = \frac{1}{2} \left(1 + \frac{e_k - \lambda_k}{E_k}\right), \quad v_k^2 = \frac{1}{2} \left(1 - \frac{e_k - \lambda_k}{E_k}\right), \quad (3.15)$$

with the quasiparticle energy

$$E_k = \sqrt{(e_k - \lambda_k)^2 + \Delta_k^2}, \quad (3.16)$$

and the pairing gap defined by

$$\Delta_k = -\frac{1}{2} \sum_{k'} \frac{(2j_{k'} + 1)^{1/2}}{(2j_k + 1)^{1/2}} u_{k'} v_{k'} G(kk k' k'; 0). \quad (3.17)$$

The QRPA equations are recovered from (3.6) by dropping the index μ and taking the limit $I^K \rightarrow 1$, substituting the unperturbed PBCS energies by the BCS energies relative to the Fermi level, defined by equation

$$E_k^{(\pm)} = \pm E_k + \lambda_k, \quad (3.18)$$

where E_k are the usual BCS quasiparticle energies defined in (3.16). In this way the unperturbed energies in (3.7) are replaced as

$$\varepsilon_{j_p}^{Z-1+\mu} + \varepsilon_{j_n}^{N-1-\mu} \rightarrow E_{j_p} + E_{j_n} + \mu(\lambda_p - \lambda_n). \quad (3.19)$$

The coefficients $X_{J_\alpha^\pi}(pn)$ e $Y_{J_\alpha^\pi}(pn)$ and the eigenvalues $\omega_{J_\alpha^\pi} (\equiv \omega)$ are given as a solution of the eigenvalues problem from the QRPA equations

$$\begin{pmatrix} \mathcal{A} & \mathcal{B} \\ \mathcal{B} & \mathcal{A} \end{pmatrix} \begin{pmatrix} X \\ Y \end{pmatrix} = \omega \begin{pmatrix} X \\ -Y \end{pmatrix}, \quad (3.20)$$

with

$$\begin{aligned} \mathcal{A}(pn p' n'; J) &= (E_p + E_n) \delta_{pp'} \delta_{nn'} \\ &+ (u_p v_n u_{p'} v_{n'} + v_p u_n v_{p'} u_{n'}) F(pn p' n'; J) \\ &+ (u_p u_n u_{p'} u_{n'} + v_p v_n v_{p'} v_{n'}) G(pn p' n'; J), \\ \mathcal{B}(pn p' n'; J) &= (v_p u_n u_{p'} v_{n'} + u_p v_n v_{p'} u_{n'}) F(pn p' n'; J) \\ &+ (u_p u_n v_{p'} v_{n'} + v_p v_n u_{p'} u_{n'}) G(pn p' n'; J). \end{aligned} \quad (3.21)$$

The eigenvalue problem in the pn-QRPA equation has the symmetry property to obtain an eigenvalue set $\pm\omega$, where the positive energies ω with eigenfunction (X, Y) represent the nucleus with $(Z+1, N-1)$, and the negative energies ω with eigenvalues (Y^*, X^*) represent the one with $(Z-1, N+1)$, where both eigenfunctions have the same absolute value norm but with different signs, as noted in Ref. [41]. Then, it is necessary to solve only one

eigenvalue equation and after that to extend the solution to the branch with the mentioned above. The perturbed energies in the pn-QRPA are defined as

$$E_\mu = \omega + \mu(\lambda_p - \lambda_n), \quad (3.22)$$

where $\mu = \pm 1$ is valid for the daughter nuclei ($Z \pm 1, N \mp 1$).

C. NME

When the excited states $|J_f\rangle$ in the final ($Z \pm 1, N \mp 1$) nuclei are described within the PQRPA, the transition amplitudes for the multipole charge-exchange operators Y_J , *etc*, listed in Table II of Ref. [21], read

$$\begin{aligned} & \langle J_f, Z + \mu, N - \mu || Y_J || 0^+ \rangle \\ &= \frac{1}{(I^Z I^N)^{1/2}} \sum_{pn} \left[\frac{\Lambda_\mu(pnJ)}{(I^{Z-1+\mu} I^{N-1+\mu}(n))^{1/2}} X_\mu^*(pnJ_f) \right. \\ & \quad \left. + \frac{\Lambda_{-\mu}(pnJ)}{(I^{Z-1-\mu} I^{N-1-\mu}(n))^{1/2}} Y_\mu^*(pnJ_f) \right], \quad (3.23) \end{aligned}$$

with the one-body matrix elements given by

$$\Lambda_\mu(pnJ) = -\frac{\langle p || Y_J || n \rangle}{\sqrt{2J+1}} \begin{cases} u_p v_n, & \text{for } \mu = +1 \\ u_n v_p, & \text{for } \mu = -1 \end{cases}. \quad (3.24)$$

In the QRPA case, using the condition $I^K \rightarrow 1$, the nuclear matrix elements for the multipole charge-exchange operators Y_J , *etc*, are

$$\begin{aligned} & \langle J_f, Z + \mu, N - \mu || Y_J || 0^+ \rangle \\ &= \sum_{pn} [\Lambda_\mu(pnJ) X_\mu^*(pnJ_f) + \Lambda_{-\mu}(pnJ) Y_\mu^*(pnJ_f)], \quad (3.25) \end{aligned}$$

with the same one-body matrix elements.

IV. COMPUTER PROGRAM AND USER'S MANUAL

The QRAP code evaluates the electron neutrino-nucleus interaction described by equation (2.1) (IREAC=1 for NS, IREAC=2 for AS) and (2.2) (IREAC=0 for MC). The processes, from the ground state of the even-even father nucleus (Z, A) to the excited states with spin (ISPIN) and parity (IPARI) in the odd-odd daughter nucleus ($Z \pm 1, A$), are calculated by using the QRPA model (IQP=0) or the PQRPA (IQP=1). These options must be setup in input data file, **grapin.dat**, which is complemented with two included files:

(a) **sp.inc**, containing the dimensions of single-particle quantum numbers, occupation probabilities, quasiparticle quantities and strength amplitudes for allowed transitions;

(b) **conf.inc**, which has the dimensions for the quasi-particle state configurations, the hamiltonian matrices (A, B) or (\mathcal{A}, \mathcal{B}) which are diagonalized, the forward and backward amplitudes, and the eigenvalues.

The input files are two: **grapout.dat**, where one can label the output file showing the neutrino/antineutrino ($\nu/\bar{\nu}$) cross section as a function of the incident neutrino, or the muon capture rate, for each state of a certain nuclear spin of the daughter nucleus; and the above mentioned **grapin.dat**, which has the quantum numbers of each single-particle state (sps) and their corresponding energy for the parent nuclei, mass and proton number of the parent nucleus, the neutron and proton pairing strengths for the BCS approximation, the strengths of particle-particle and particle-hole of residual interaction, the position of the Fermi level and the experimental gap for neutron and proton, ; and finally the Q -value for the $\nu/\bar{\nu}$ scattering.

There are three default output files. Two of them, **AUXI.out** and **OUT.out**, contain the results of the nuclear structure model, whereas the results for the weak processes appear in the file created by **grapout.dat**. For example, if one is interesting in the multipole $J^\pi = 1^+$ with a single-particle space of six levels in ^{12}C (“*set 1*”), we can introduce in **grapout.dat** the file names **QNC.out** (**PNC.out**) for neutrino capture, **QAC.out** (**PAC.out**) for antineutrino capture, **QMC.out** (**PMC.out**) for muon capture, using the QRPA (PQRPA) model. All the mentioned output are included as examples. The output neutrino or antineutrino-nucleus cross sections are given in 10^{-42}cm^2 with the energies in MeV and the muon capture rate in 10^4s^{-1} .

A. Reading the data

There are three sets of input in **grapin.dat** separated in modules labeled as: **Data set 1* for a single-particle space of six levels in ^{12}C (0, 1 and 2 $\hbar\omega$ oscillator shells), **Data set 2* for a single-particle space of ten levels in ^{12}C (0, 1, 2 and 3 $\hbar\omega$ oscillator shells), and **Data set 3* for single-particle space of 12 levels in ^{56}Fe (2, 3 and 4 $\hbar\omega$ oscillator shells).

For each one of these input data, the number of sps represents the available space where one wants to solve the BCS (or PBCS) problem given by equations (3.13) and (3.14) ((3.1)-(3.2)). It contains the necessary number of harmonic oscillator shells leading to a smooth smearing of the Fermi surface. The Fermi level with the neighboring levels constitute the active shell for the smearing of the Fermi's surface. For example, in ^{12}C (ground state with $J = 0^+$) the active shell is composed by the $1p_{3/2} - 1p_{1/2}$ levels. The last nucleons according to the single-particle model are in $1p_{3/2}$ and it could be promoted to the $1p_{1/2}$, creating a particle state in $1p_{1/2}$ and a hole state in $1p_{3/2}$. This scheme describes the first particle-hole (ph) excitation on ^{12}C in order to obtain the ^{12}N or ^{12}B ground

state with $J = 1^+$ if one promotes a proton or a neutron to the $1p_{1/2}$ level.

Let us show as example a data input of six sps for ^{12}C : **Data set 1*. The rows starting with a symbol “*” are not read as input and serves only to remind the user the meaning of the physical quantities. Taking out the comments “*” of this file, we have

```

1 +1 0.0 1 1
06 06 0 1 1 0
101 -20.09 112 -6.02 111 -0.29 123 3.07 201 3.85 122 7.18
101 -18.19 112 -3.17 111 2.79 123 5.73 201 6.06 122 9.36
12 06 28.80 28.85 30.0 50.0 27.0 64.0
2 1 6 6 1.00 6.88
2 1 6 6 1.00 7.00

```

First line: Nuclear spin (ISPIN=1) of the daughter nucleus, parity (IPARI=+1), coupling strength of particle-particle channel ($t = 0.0$) (see definition below), index of neutrino reaction (IREAC=1) and the index (IQP=1) to solve the PQRPA problem.

Second line: Number of neutron sps (NSN=06), number of proton sps (NSP=06), index to solve the QRPA equation in the Tamm-Damcoff approximation (ITD: 0 no, 1 yes), index to print the matrix elements of the nuclear hamiltonian to be diagonalized (MAPR: 0 no, 1 yes), index to solve the BCS equation with the self-energy term (IFMU: 0 no, 1 yes), index to make the RPA matrix with the branch ($Z+1, N-1$) ($\mu = 1$) or ($Z-1, N+1$) ($\mu = -1$) of PQRPA (IPRO: 0($\mu = 1$), 1($\mu = -1$)).

Second and Third lines: quantum numbers and single particle energies (s.p.e.) of each sps for neutrons and protons, correspondingly. These are represented in the same way as in the shell model scheme, with their respective quantum numbers ($n \ell (j + \frac{1}{2})$). For example $101 \rightarrow 1s_{1/2}$ where 1 is principal quantum number, corresponding to the first harmonic oscillator level (n), 0 corresponds to the angular orbital momentum $\ell \equiv s$ and the last number $1 \equiv j + \frac{1}{2} = \frac{1}{2} + \frac{1}{2}$ represents the total angular momentum ($j = \ell + m_s$) as a sum of angular momentum ($\ell = 0$) plus the spin projection ($m_s = \frac{1}{2}$) adding a constant value of $\frac{1}{2}$ to obtain a integer number. Table I shows the notation and the corresponding quantum numbers.

Fourth line: Mass number (IAM=12), proton number (IZ=6), pairing coupling constant for neutron v_s^{pairN} (VspairN=28.80) and proton v_s^{pairP} (VspairP=28.85), v_s^{pp} pairing coupling constant for the particle-particle (pp) singlet channel (VsPP=30), v_t^{pp} pairing coupling constant for the pp triplet channel (VtPP=50), and v_s^{ph} pairing coupling constant for the particle-hole (ph) singlet channel (VsPH=27), and finally v_t^{ph} pairing coupling constant for the ph triplet channel (VtPH=64).

Fifth and Sixth lines: Position of the Fermi level (LEVEL=2), initial (IIQ=1) and final (IFQ=6) states for which the BCS equations must be solved, number of particles interacting (NPIQ=6) in these levels and the experimental gap (DELTAQ=6.88 or 7.00) defined below in equation (4.2); for neutrons and protons, fifth and

TABLE I: Notation for the quantum numbers, the resulting single-particle energies e_j^N for neutrons and e_j^Z for protons, and the pairing strength v_s^{pair} within the BCS. The energies are given in units of MeV, and v_s^{pair} is dimensionless.

Notation	Shell	n	ℓ	$j + 1/2$	e_j^N	e_j^Z
101	$1s_{1/2}$	1	0	1	-20.09	-18.19
112	$1p_{3/2}$	1	1	2	-6.02	-3.17
111	$1p_{1/2}$	1	1	1	-0.29	2.79
123	$1d_{5/2}$	1	2	3	3.07	5.73
201	$2s_{1/2}$	1	0	1	3.85	6.06
122	$1d_{3/2}$	1	2	2	7.18	9.36
v_s^{pair}					28.80	28.85

TABLE II: Parity and nuclear spin for the states obtained in the nucleus with the one-quasiparticle space used in the input for ^{12}C .

	$1s_{1/2}$	$1p_{3/2}$	$1p_{1/2}$	$2s_{1/2}$	$1d_{5/2}$	$1d_{3/2}$
$1s_{1/2}$	$0^+, 1^+$					
$1p_{3/2}$	$1^-, 2^-$	$0^+, 1^+$ $2^+, 3^+$				
$1p_{1/2}$	$0^-, 1^-$	$1^+, 2^+$	$0^+, 1^+$			
$2s_{1/2}$	$0^+, 1^+$	$1^-, 2^-$	$0^-, 1^-$	$0^+, 1^+$		
$1d_{5/2}$	$2^+, 3^+$	$1^-, 2^-$ $3^-, 4^-$	$2^-, 3^-$	$2^+, 3^+$	$0^+, 1^+, 2^+$ $3^+, 4^+, 5^+$	
$1d_{3/2}$	$1^+, 2^+$	$0^-, 1^-$ $2^-, 3^-$	$1^-, 2^-$	$1^+, 2^+$	$1^+, 2^+$ $3^+, 4^+$	$0^+, 1^+$ $2^+, 3^+$

sixth lines respectively.

Seventh line: Q -value minus the lepton mass for $\nu/\bar{\nu}$ scattering (EGS=17.338 for ^{12}N [42]). It can be adopted as the energy of the ground state of daughter nucleus. The lepton mass must be added to EGS to obtain the Q -value for the reaction.

B. Running the code

QRAP solves as first step the BCS problem. In this case, one needs to adjust the pairing strength to reproduce the experimental pairing gap. After that, one can solve the PBCS problem or directly the QRPA if the option IQP=0 was selected. If IQP=1 then the PQRPA equations are solved. It means that QRAP firstly calculates the nuclear matrix elements in the QRPA or PQRPA by selecting the option IQP=0 or 1, appropriately. The option of which type of weak interaction processes one wants to evaluate is adopted with IREAC in the input data. We recommend first to adjust the pairing strength as it explained below. After this it is convenient to fit the parameters of the residual interaction using the option IREAC=3 for the muon capture rate because this calculation is fast. Physically you can check quickly how

good is your adoption of parameters because the inclusive muon capture rate and $B(GT)$ strength are values available in the literature (see for example Refs. [43, 44]).

For the residual interaction the code assumes a delta force,

$$V = -4\pi (v_s P_s + v_t P_t) \delta(r), \quad (4.1)$$

which has been used extensively in the literature [25, 26, 27] to describe single and double beta decays.

Next, we explain how the parameters of the interaction are adjusted using for example the input data for six levels in ^{12}C . The results are presented in output file **OUT.out**.

• Adjusting the gap Δ_k :

The parameters v_s^{pairN} and v_s^{pairP} are adjusted to reproduce the experimental gap Δ^N for neutrons and Δ^Z for protons solving the BCS equations (2.33) and (3.5) in a self-consistent way. The experimental gap, according the equation (2.96) of Bohr-Mottelson, Vol. I [45], are:

$$\begin{aligned} \Delta^N &= -\frac{1}{2} \{ \mathcal{B}(N-1, Z) - 2\mathcal{B}(N, Z) + \mathcal{B}(N+1, Z) \}, \\ \Delta^Z &= -\frac{1}{2} \{ \mathcal{B}(N, Z-1) - 2\mathcal{B}(N, Z) + \mathcal{B}(N, Z+1) \}, \end{aligned} \quad (4.2)$$

where $\mathcal{B}(N, Z)$ is the binding energy of the even-even nucleus $A(Z, N)$. This is the most common fit (Fit1) used in several works with usual QRPA [27, 28, 29]. In this case, the $\Delta^{N(Z)}$ must be equal or approximately the $\Delta_{j_k=FL}^{N(Z)}$ corresponding to the Fermi level (FL). To solve the set of PBCS coupled equations for u_k and v_k (3.15) is recommended that you first obtain the solutions for the BCS problem because these probability occupation are use as input for the PBCS case. The PBCS coupled nonlinear equations are solved consistently with Powell Hybrid method using subroutine HYBRD [46].

The results of the BCS or PBCS problem are shown as tables in the first lines of **OUT.out** for neutrons and protons, respectively. The quantities defined by (3.9) and (3.10) are presented there. In particular the projected quasiparticle energy defined in (3.9) are

$$\text{PROYSP} = \begin{cases} E(+) = \epsilon_k^K, & \text{with } k \text{ above Fermi level,} \\ E(-) = \epsilon_k^{K-2}, & \text{with } k \text{ below Fermi level,} \end{cases} \quad (4.3)$$

means that $E(+)$ corresponds to a particle state and $E(-)$ to a hole state. The values of $\Delta_{j_k}^{N(Z)}$ are shown in the ninth column of the table labeled CONFIGURATION SPACE. This Fit1 was based in that the difference between the experimental energy levels above ($E_p \equiv$ particle level) and below ($E_h \equiv$ hole level) is approximately twice the experimental gap, *i.e.*,

$$E_p^K - E_h^K \simeq 2\Delta^K, \quad (4.4)$$

with $K = N$ or Z .

There is another adjustment procedure for the pairing gap called by Fit2. In Fit2, all the single particles energies $e_j^{N(Z)}$ from Table I are varied with a χ^2 search to account for the experimental spectra E_j :

$$\begin{aligned} \epsilon_k^{Z(N)} &\rightarrow E_p^{Z(N)} \equiv E(+), & \text{for a particle state,} \\ \epsilon_k^{Z-2(N-2)} &\rightarrow E_h^{Z(N)} \equiv E(-), & \text{for a hole state.} \end{aligned}$$

With Fit 2, the equation (4.4) is already satisfied. This procedure was employed to obtain the e_j spectra of Table III in Ref. [21]. Whereas the e_j for the reduced space of six levels of the present example are shown in Table I. These are the s.p.e. of input data *Data set 1*.

To avoid introducing more effort in the calculations, the Fit1 procedure is the usual choice, with the e_j spectra obtained either from a harmonic oscillator or from a Wood-Saxon potential, and the v_s^{pairN} and v_s^{pairP} being varied to satisfy $\Delta_{j_k=FL}^{N(Z)} \approx \Delta^{N(Z)}$.

For ^{56}Fe the input data is called **Data set 3*. The s.p.e of the active $3\hbar\omega$ shell were adopted from the experimental energies of ^{56}Ni , and the $2\hbar\omega$ and $4\hbar\omega$ shells were taken from the harmonic oscillator energies with $\hbar\omega/\text{MeV} = 45 A^{1/3} - 25 A^{2/3}$. Fit1 was employed to adjust the experimental $\Delta^{N(Z)}$ for ^{56}Fe .

• Adjusting the parameters of particle-hole strength

In general v_s^{ph} and v_t^{ph} could be taken from a systematic study from the GT resonances as done in Ref. [47] (see also Ref. [39]). In the input data, these parameters were fixed to $v_s^{ph} = 27$ and $v_t^{ph} = 64$ (in MeV fm^3), previously fitted for ^{48}Ca , and shown to yield a good description of double beta decay.

To analyze the behavior of theoretical observables with respect to some experimental value, whenever possible, it is convenient to use the new set of parameters

$$\begin{aligned} r &= \frac{v_s^{ph} + v_t^{ph}}{v_s^{pair}(p) + v_s^{pair}(n)} \\ p &= \frac{3v_t^{ph} - v_s^{ph}}{v_s^{pair}(p) + v_s^{pair}(n)}. \end{aligned} \quad (4.5)$$

In the ^{12}C nucleus, the ground state of ^{12}N and their $B(GT)$ were adopted to select these parameters. Some previous work on RPA calculations on ^{12}C in Ref. [48] uses the relation

$$v_t^{ph} = v_s^{ph}/0.6, \quad (4.6)$$

to estimate the triplet ph depth. Additionally, it is reasonable to adopt a singlet ph strength that is the same as v_s^{pair} obtained from the proton and neutron gap equations, *i.e.*,

$$v_s^{ph} = v_s^{pair}. \quad (4.7)$$

Fig. 1 shows the behavior of the ground state energy of ^{12}N and the $B(GT)$ strength as a function of the parameters (r, p) defined in equation (4.8) using the *Data*

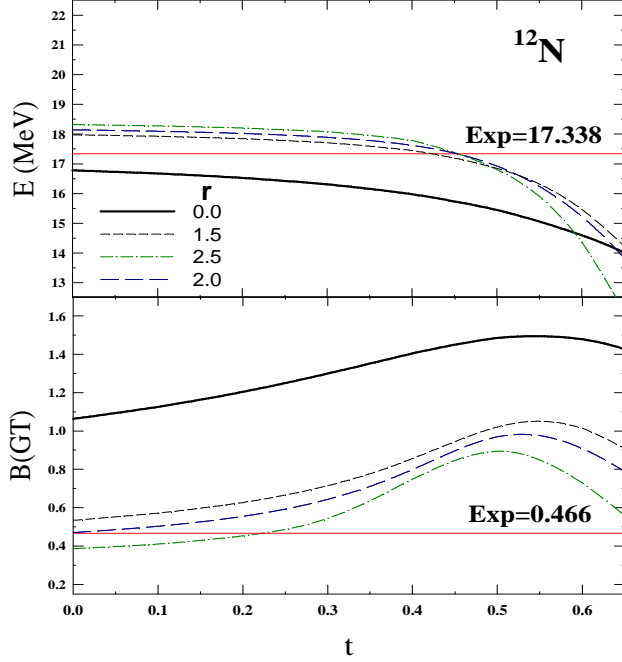


FIG. 1: Comparison of the ground state energy $E \equiv E(^{12}\text{N}_{gs})$ and $B(GT)$ -value with different parametrizations r in the ph -channel as a function of t parameter of the pp -channel. The experimental values [42, 49, 50] are also shown. $r = 2$ corresponds to $v_s^{ph} = 27$ and $v_t^{ph} = 64$ (Case PII of [21]). The *Data set 2* was employed.

set 2. We note from Fig. 1 that increasing the r -values is possible to find a set, which allows that the ground state energy E and the theoretical strength $B(GT)$ be close to the experimental values. This analysis must be done at the same time to observe the variation of E and $B(GT)$, with respect of the t -value for the pp -channel.

• Adjusting the parameters of particle-particle strength

In general, the pp -strengths are fixed based on the $SU(4)$ and isospin symmetry as $v_s^{pp} \equiv v_s^{pair}$, and $v_t^{pp} \gtrsim v_s^{pp}$ for nuclei with $N > Z$. It is more convenient to work with another set of parameters related to (v_s^{pp}, v_t^{pp}) coupling strengths in the pp channel ($T = 1, S = 0$) and ($S = 1, T = 0$) for the matrix elements G of equation (3.5):

$$\begin{aligned} s &= \frac{2v_s^{pp}}{v_s^{pair}(p) + v_s^{pair}(n)}, \\ t &= \frac{2v_t^{pp}}{v_s^{pair}(p) + v_s^{pair}(n)}. \end{aligned} \quad (4.8)$$

It was shown in Ref [19] that for ^{12}C the above parametrization $v_s^{pp} \equiv v_s^{pair}$ and $v_t^{pp} \gtrsim v_s^{pp}$ might not be suitable for $N=Z$. In fact, the best agreement with data in ^{12}C was obtained when the pp -channel is totally switched off, *i.e.*, $v_s^{pp} \equiv v_t^{pp} = 0$, and three different set of values for the ph coupling strengths were used. These conditions are related with $s = t$ for ^{12}C ($N=Z$), and $s = 1$ and t variable in nuclei with $N > Z$. In ^{56}Fe the values $s = 1$ and $t = 0$ were adopted. In the code QRAP

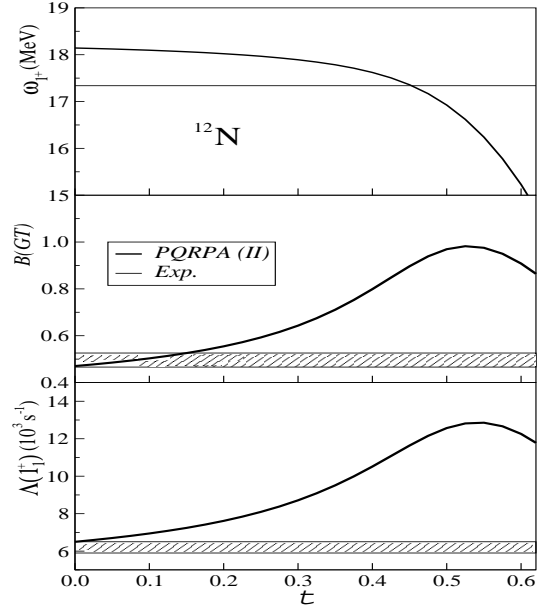


FIG. 2: Results from PQRPA calculations shown in Ref. [21], as a function of the pp parameter t , compared with the experimental data taken from Refs. [42, 49, 50] for: (i) energy difference ω_{1+} between the 1^+ ground state in ^{12}N and the 0^+ ground state in ^{12}C (upper panel), (ii) $B(GT)$ -value for the β transition between these two states (middle panel), and (iii) exclusive muon capture rate $\Lambda(1^+)$ (lower panel). The parameters of the ph channel for the δ -interaction are $v_s^{ph} = 27$ and $v_t^{ph} = 64$.

the following conditions are standard: (i) $s = t$ with t as a variable parameter for $N=Z$; and (ii) $s = 1$ and t as a variable parameter for $N > Z$, *i.e.*, the residual interaction is defined as a function of two adjustable parameters v_t^{ph} and t .

Some observables could be used as set of data available in the literature to check the adoption of the residual interaction parameters for a particular nucleus. For example, the ground state energy of daughter nucleus and the $B(GT)$ strength for the β^+ or β^- decay, or partial muon capture rate [19, 21, 51] can be used. Fig. (2) shows the behavior of the ground state energy in ^{12}N with respect to ^{12}C , ω_{1+} , $B(GT)$, and the exclusive muon capture rate Λ_{1+} , as a function of the parameter t . These results were presented in Ref. [21]. The t parameter of pp -channel is related with the known collapse problem in RPA-like models [24, 25, 26].

We can use the reduced space of six levels to identify in the output file, the quantities shown in Fig. 1. Here, we use three values of t and the results are shown in Table III for relevant observables.

The ω_{1+} and $B(GT)$ can be extracted from the output file **AUXI.out**. This file shows the Ikeda sum rule when $J^\pi = 0^+$ or 1^+ with the total amplitude strength for β^- -decay: $S(+)/3$, and for β^+ -decay: $S(-)/3$. For the PQRPA case, we also show: the unperturbed energy, left

TABLE III: Evolution of ground state energy, $B(GT)$ and exclusive muon capture rate in ^{12}C as function of the pp -channel parameter t . With [a] and [b] we denotes the output file “AUXI.out” and “PMC.out”. ω_{1+} is in MeV, $B(GT)$ dimensionless and (Λ_{1+}, Λ) in 10^4 s^{-1} . The parameters for the ph -channel are $(v_s^{PH} = 27, v_t^{PH} = 64)$.

	State [File]	Obs.	t			
			0.0	0.3	0.6	Exp.
^{12}N	16 [a]	ω_{1+}	18.319	17.951	14.970	17.34 [42]
	16 [a]	$B(GT)$	0.496	0.696	0.840	0.466 [49]
^{12}B	17 [a]	ω_{1+}	12.528	12.126	9.202	13.36 [42]
	17 [a]	$B(GT)$	0.502	0.693	0.837	0.526 [49]
	16 [b]	Λ_{1+}	0.695	0.936	1.119	0.62(3) [50]
	[b]	$\Lambda (1^+)$	1.722	1.537	1.183	

side of equation (3.19), for the $Z + 1$ daughter nucleus with $\mu = +1$, and with $\mu = -1$ for $Z - 1$ daughter nucleus. Using the example *Data set 1*, we have generated NC=16 states 1^+ for ^{12}N and ^{12}B obtained through the PQRPA (QRPA) on the even-even ^{12}C nucleus.

The ground state corresponds to IN=16 labeled as STATE 16 in the first column corresponding to the state number in the Table that appears in **AUXI.out**. For this table, the second and third columns are the non-perturbed energies (PBCS energies) of the $(Z \pm 1, N \mp 1)$ nuclei, respectively. The third column shows the perturbed energies of the $(Z+1, N-1)$ nuclei (^{12}N) from STATE=1 to STATE=NC(=16), and next in the same column the (minus) perturbed energies of the $(Z-1, N+1)$ nuclei (^{12}B) are listed from state NC+1(=17) to state 2NC(=32). Note that NC=16 corresponding to the ground state energy for nucleus $(Z+1, N-1)$ and the ground state energy for nucleus $(Z-1, N+1)$ (with positive value) corresponds to the state [NC+1]=17.

The fifth (SP0) (β^-) and sixth (SN0) (β^+) columns are the non-perturbed B -values (F or GT) (PBCS). The seventh (SPP) and eighth (SNP) columns are the perturbed B -values, (β^-) and (β^+). We see that the main non-perturbed $B(GT)$ (or $B(F)$) strength corresponds to STATE=6 (STATE=5) of the unperturbed energy En+1 (En-1). In these unperturbed states, the state STATE=6 has the configuration $(1p_{1/2}^\pi, 1p_{3/2}^\nu)$ (1 particle in proton, 1 hole in neutron) for ^{12}N , and the STATE=5 in ^{12}B has the configuration $(1p_{3/2}^\pi, 1p_{1/2}^\nu)$ (1 particle in neutron, 1 hole in proton). For the perturbed $B(GT)$ (or $B(F)$) strength, the main contribution corresponds to the state NC(=16) for the nucleus $(Z+1, N-1)$, whereas that in the nucleus $(Z-1, N+1)$ corresponds to state [NC+1]=17. These perturbed states have the 1p-1h configurations as main component in the wave function, *i.e.*, the particle-hole limits for the seniority two- pn states as it was shown and discussed in Ref. [21].

If the spin state of the daughter nucleus, J^π , is different

of 1^+ or 0^+ , the unperturbed and perturbed energies are only shown in **AUXI.out**.

In the output file **OUT.out** are displayed the PBCS or BCS results. This file also shows, with the option MAPR= 0, the matrix elements $(\mathcal{A}, \mathcal{B})$ eq. (3.22) for the QRPA, or $(A_{\mu=1}, B)$ eq. (3.7) for PQRPA. In the next explanations the numbers that appears parenthetically are results with *Data set 1* for the multipole $J^\pi = 1^+$. The nuclear wave functions are also written in this output file. They are labeled for each state of the multipole evaluated, from IN=1 (state with highest energy) to the IN=NC(=16)(state with lowest energy) for the nucleus $Z+1$ (^{12}N), and for IN=NC+1(=17) (state with lowest energy) to the IN=2NC(=32) (state with highest energy) for the nucleus $Z-1$ (^{12}B). If we print out results for QRPA, the wave functions are extended only to IN=NC (state with lowest energy). For ^{12}N and ^{12}B the lowest state IN=NC (16 and 17) with $J^\pi = 1^+$ corresponds to ground state.

The wave functions table for PQRPA has subsequently in the 1st, 2nd, 3rd columns the single particle state component, and the state configuration of neutron-proton (CONFIGUR); 4th column (UNP.EN+1) and 5th column (UNP.EN-1) the unperturbed energies for the nucleus $Z \pm 1$; 6th and 7th column the perturbed energies (PERT.ENER) ($\omega_{\mu=1}, -\omega_{\mu=-1}$) for the nucleus $(Z+1, Z-1)$; and in the next 8 columns (arranged in four pairs) labeled by IN the wave functions components $(X(pnJ_f), Y(pnJ_f))$ for IN=1 to IN=NC(=16) for the nucleus $Z+1$ (^{12}N); and for IN=NC+1(=17) to IN=2NC(=32) the components $(Y(pnJ_f), X(pnJ_f))$ for the nucleus $Z-1$ (^{12}B).

For example, from PMC.out (muon capture in ^{12}C with $J^\pi = 1^+$) in the part OUT.out, the ground state is IN=16 with the main forward amplitude $X(pnJ_f) = 0.963$ (backward $Y(pnJ_f) = 0.003$) corresponding to the CONFIGUR 6 112 111, *i.e.*, single particle state number 6 with configuration $(1p_{3/2}^\nu - 1p_{1/2}^\pi, 1^+)$ with non-perturbed energy (16.78) and perturbed energy (18.32) shown at the foot of table.

For the QRPA printing, we have in the 1st, 2nd, 3rd column the state configuration (CONFIGUR); 4th column (UNP.ENER) unperturbed energy; 5th column (PERT.ENER) the perturbed energy ω (3.14) for both nuclei $Z \pm 1$. In this case, the same wave function IN, changing the forward $X(pnJ_f)$ and backward $Y(pnJ_f)$ components, corresponds to the nucleus $Z \pm 1$ with eigenenergies described by eq.(3.14). If $J^\pi = 1^+$ or 0^+ , the perturbed B -strength S(+) and S(-) are shown in rows for the last table (PER. STRENGTHS) in **OUT.out** file.

Table III shows the ground state energy, $B(GT)$ and exclusive muon capture rate for ^{12}N and ^{12}B obtained for $t = 0.0, 0.3$ and $t = 0.6$ in comparison with the experimental data.

- Output for the ν -nucleus processes

With the pairing and residual interaction conveniently parameterized, it is possible to obtain some results for

ν -nucleus processes. We obtain the output for weak processes according to the option **IREAC**:

IREAC=0 prints the results for the muon capture rate in the file (QMC.out or PMC.out). They are shown in the table labeled CAPTURE RATE in the following order: first column is the IN state, 2nd col. the muon capture rate R.CAPTURA in 10^4 s^{-1} , 3rd. col. the perturbed energy E(Z-1) in MeV for the nucleus Z-1, 4th. col. the perturbed B^+ -strength SNP, 5th col. the perturbed energy E(Z+1) in MeV, 6th col. the perturbed B^- -strength. The B^\pm -strengths are only shown for the allowed transitions. The total muon capture for the spin J^π is printed in the last row.

If the nuclear spin is 1^+ or 0^+ the folded strength

$$S^\pm(E) = \frac{1}{\pi} \sum_{pn} |\langle J_f, Z \pm 1, pn | \hat{O}^\pm | J_i \rangle|^2 \frac{\eta}{\eta^2 + (E - \omega_\mu)^2}, \quad (4.9)$$

is sketched in this output file. Here, \hat{O}^\pm is the Fermi or Gamow-Teller operator and $\eta = 1 \text{ MeV}$. If the nuclear spin is different from 1^+ or 0^+ the $S^\pm(E)$ are not shown.

IREAC=1 or **IREAC=2** prints the results for the neutrino or antineutrino cross sections in the files (QNC.out/PNC.out) or (QAC.out/PAC.out). The cross sections (SIGMA(ENU)) are calculated as a function of the neutrino energy (ENU) for each state of the nuclear spin from IN=1 to IN=NC. The absolute value of maximum ($\cos\theta=-1$) and minimum ($\cos\theta=1$) nuclear momentum transfer for each energy are also printed. If the nuclear spin is 1^+ or 0^+ , the folded strength $S^\pm(E)$ is also printed.

Note: The cross section results are printed up to a maximum energy of 300 MeV. Depending upon the single particle space employed, the cross sections as a function of the neutrino energy must be restricted to lower energies ($E_\nu < 100 \text{ MeV}$) to satisfy the energy-weighted sum rules. This interval of energies is important for supernova neutrinos and low-energies decay-at-rest neutrinos [10].

V. ROUTINES INCLUDED WITH THE CODE

QRPA solves the pn -QRPA or pn -PQRPA charge-exchange problem for a nuclear spin J^π of the daughter odd-odd nucleus.

SUAVE calculates and prints the folded strength $S^\pm(E)$ in equation (4.9), folding the B -strength with a Lorentzian function with $\eta = 1 \text{ MeV}$.

RMUONCAP calculates the muon capture rate given by formula (2.29).

SIMPSN2 calculates the neutrino or antineutrino cross sections as a function of the neutrino energy. This subroutine uses the function **G** to call the subroutine **SECCION**, which evaluates the cross section formula (2.23) using the Gauss-Legendre N-point quadrature formula [52] on the function **F** to evaluate the angular integration of the transition amplitude times E_ℓ .

MATRIXP computes the matrix elements with the delta residual interaction given in Ref. [53] for the PQRPA. The matrix elements were modified according to the projection procedure shown in equation (3.7).

MATRIX computes the matrix elements with the delta residual interaction given in Ref. [53] for the QRPA. The matrix elements are shown in equations (3.21).

RPA finds eigenvalues and eigenvectors for the QRPA or PQRPA equations. It uses the subroutine **EIGRF** and other related subroutines of the IMSL Library [54] to orthonormalize the eigenvectors.

GAPII solves the set of BCS coupled equations (3.13) and (3.14) to obtain the v_i^t s and u_i^t s for neutrons and protons independently.

CONFGT prepares configurations for states with a given spin and parity.

FAUX evaluates the matrix elements G and F equation (3.17) for $J^\pi = 0^+$ using a delta interaction for neutrons and protons independently.

RADWF computes harmonic oscillator radial wave functions. It uses the additional subroutine **OSCILL** to evaluate the radial coefficients.

HYBRD finds a zero of a system of N nonlinear equations in N variables by a modification of the Powell Hybrid method. This subroutine was provided by the Argonne National Laboratory [46]. It uses the subroutine **FCN** to calculate the PBCS nonlinear equations given by formula (3.1).

FKPERMAT evaluates the perturbed projected matrix elements for the beta decay operator for $\mu = 1$ and $\mu = -1$ respectively, according eqs. (3.23) for PQRPA, and (3.25) for QRPA. The radial part of the SPNME were defined in Ref. [55]. This subroutine uses the subroutine **ANGULARMATRIX** to calculate the angular part of single-particle matrix elements defined in Ref. [56] and shown in the Appendix for the sake of completeness.

There are other routines in the code shortly described as follows. **PRINMA** prints the matrix elements (\mathcal{A}, \mathcal{B}) for the QRPA, or (A_μ, B) for PQRPA, **SKIPCOM** is used to skip comments in the input file, **UNPMOM3** evaluates the unperturbed projected matrix elements for beta decay, **BETMAT2** is used to calculate the single-particle matrix elements for beta decay, **PROENER** calculates the quantities for the projected quasiparticles energies in (3.23)

VI. THINGS TO DO

1. Use the sample input *Data set 1* to obtain the results presented in Table III.
2. Modify the input *Data set 1* by *Data set 2*, setting all parameters of the residual interaction to zero. These values correspond to BCS or PBCS approximation. Compare the folded strength of *Data set 1* with *Data set 2* shown in fig. 4 of Ref. [21].
3. In Ref. [57] the s.p.e. for neutrons were changed to analyze the systematics of the pairing strength in the odd

carbon isotopes. Change the s.p.e for neutrons in *Data set 2* and reproduce the systematics shown in the level scheme of fig. 2 and the spectroscopic factors of fig. 3 of Ref. [57].

Acknowledgments

This work was partially supported by the U.S. DOE grants DE-FG02-08ER41533 and DE-FC02-07ER41457 (UNEDF, SciDAC-2), and the Research Corporation under Award No. 10497. F.K. thanks the financial aid of the CONICET-Argentina. A.R.S. wish to express their sincere thanks to C.A. Barbero and A.E. Mariano for help received in programming the s.p. matrix elements.

Appendices

A. Single-particle nuclear matrix elements

The elementary operators defined in equation (2.16) have the reduced single-particle pn matrix elements (RSPME) defined in [35, 56] (Let us remember that $\kappa = |\mathbf{k}|$ and $\mathbf{p} = -i\nabla$).

For the RSMPE dependent of the tensor product of spherical harmonic times the nucleon velocity we have

$$\langle p, (l_p \frac{1}{2}), j_p || j_L(\kappa r) [Y_L(\hat{\mathbf{r}}) \otimes \nabla]_J || n, (l_n \frac{1}{2}), j_n \rangle = \frac{(-1)^{1+J+L}}{\sqrt{4\pi}} \left[W_{LJ}^{(-)}(pn) R_L^{(-)}(pn; \kappa) + W_{LJ}^{(+)}(pn) R_L^{(+)}(pn; \kappa) \right], \quad (6.1)$$

with angular and radial

$$W_{LJ}^{(\pm)}(pn) = \pm (-1)^{l_p+j_n+J+1/2} \hat{J} \hat{l}_p \hat{j}_p \hat{j}_n (l_n + \frac{1}{2} \mp \frac{1}{2})^{1/2} (l_p L | l_n \mp 1) \left\{ \begin{matrix} l_p & j_p & \frac{1}{2} \\ j_n & l_n & J \end{matrix} \right\} \left\{ \begin{matrix} L & J & 1 \\ l_n & l_n \mp 1 & l_p \end{matrix} \right\},$$

$$R_L^{(\pm)}(pn; \kappa) = \int_0^\infty u_{n_p, l_p}(r) \left(\frac{d}{dr} \pm \frac{2l_n + 1 \pm 1}{2r} \right) u_{n_n, l_n}(r) j_L(\kappa r) r^2 dr, \quad (6.2)$$

parts, respectively. We use here the angular coupling $|(l_p, j_p), J \equiv \sqrt{2J+1}$ and $(l_p L | l_n \mp 1)$ is the short notation for the Clebsh-Gordon coefficient $(l_p 0 L 0 | (l_n \mp 1) 0)$.

For the scalar product of spin times nucleon velocity, we have

$$\langle p, (l_p \frac{1}{2}), j_p || j_J(\kappa r) Y_J(\hat{\mathbf{r}}) (\boldsymbol{\sigma} \cdot \nabla) || n, (l_n \frac{1}{2}), j_n \rangle = \frac{1}{\sqrt{4\pi}} \left[W_J^{(-)}(pn) R_J^{(-)}(pn; \kappa) + W_J^{(+)}(pn) R_J^{(+)}(pn; \kappa) \right], \quad (6.3)$$

with the angular part

$$W_J^{(\pm)}(pn) = \pm (-1)^{l_n+j_n+J+1/2} \sqrt{6} \hat{J} \hat{l}_p \hat{j}_p \hat{j}_n (l_n + \frac{1}{2} \mp \frac{1}{2})^{1/2} (l_p J | l_n \mp 1) \left\{ \begin{matrix} 1 & \frac{1}{2} & \frac{1}{2} \\ j_n & l_n & l_n \mp 1 \end{matrix} \right\} \left\{ \begin{matrix} l_n \mp 1 & j_n & \frac{1}{2} \\ j_p & l_p & J \end{matrix} \right\}, \quad (6.4)$$

being the radial part $R_J^{(\pm)}(pn; \kappa)$ as in (6.2).

The RSPME of the two operator independent of the nucleon velocity are written below. For the spherical Bessel function times the spherical harmonic, we have

$$\langle p, (l_p \frac{1}{2}), j_p || j_J(\kappa r) Y_J(\hat{\mathbf{r}}) || n, (l_n \frac{1}{2}), j_n \rangle = \frac{1}{\sqrt{4\pi}} W_{J0}(pn) R_J^0(pn; \kappa), \quad (6.5)$$

with the angular and radial

$$W_{J0}(pn) = (-1)^{j_p-j_n} \hat{J} \hat{j}_p \hat{j}_n \begin{pmatrix} j_p & j_n & J \\ \frac{1}{2} & -\frac{1}{2} & 0 \end{pmatrix}, \quad (6.6)$$

$$R_J^0(pn; \kappa) = \int_0^\infty u_{n_p, l_p}(r) u_{n_n, l_n}(r) j_J(\kappa r) r^2 dr,$$

parts, respectively. And finally, the RSMPE dependent of the tensor product of spherical harmonic times the spin operator reads

$$\langle p, (l_p \frac{1}{2}), j_p || j_L(\kappa r) [Y_L(\hat{\mathbf{r}}) \otimes \boldsymbol{\sigma}]_J || n, (l_n \frac{1}{2}), j_n \rangle = \frac{(-1)^{L+1+J}}{\sqrt{4\pi}} W_{LJ}(pn) R_L^0(pn; \kappa), \quad (6.7)$$

with the angular

$$W_{LJ}(pn) = (-1)^{l_p} \sqrt{6} \hat{j}_p \hat{j}_n \hat{l}_p \hat{l}_n \hat{J} \hat{L} \hat{J} \begin{pmatrix} l_p & L & l_n \\ 0 & 0 & 0 \end{pmatrix} \left\{ \begin{matrix} \frac{1}{2} & l_p & j_p \\ \frac{1}{2} & l_n & j_n \\ 1 & L & J \end{matrix} \right\}, \quad (6.8)$$

with the $R_L^0(pn; \kappa)$ radial part of (6.6).

B. On the Fermi function and EMA

The QRAP code is setup to use by default the Fermi function to take into account the Coulomb interaction of the lepton with the residual nucleus. This condition was employed by several works for reactions on ^{12}C with neutrinos from the DAR of μ^+ . As claimed in Ref. [23], the quantity $p_\ell R_A$ is of the order of 0.5, where R_A is the radius of the nucleus. Thus, the situation is well described by a Fermi function. Moreover, for high energy neutrinos, e.g. neutrinos from the DIF of π^+ , the outgoing muons have $p_\ell R_A > 0.5$. With these *relativistic* leptons, the effective momentum approximation (EMA) [58] takes care of the Coulomb field of the daughter nucleus, instead of the Fermi function. This condition is adopted in the code within the subroutine SECCION: with EMA=0 the Fermi function is adopted, and with EMA=1 the EMA prescription. In the EMA procedure, the lepton energy and momentum are modified by a constant electrostatic potential within the nucleus

$$E_{\ell,eff} = E_\ell - V_{eff},$$

$$p_{\ell,eff} = \sqrt{E_{\ell,eff}^2 - m_\ell^2},$$

with $V_{eff} = 4V_C(0)/5 = -6Z_f\alpha/5R_A$ [32, 59]. These two prescriptions for the Coulomb correction were tested

in the calculation of the inclusive cross section for neutrino scattering on ^{208}Pb [32]. As shown in Ref.[32], the Fermi function correction overestimates the cross sections coming from EMA at higher neutrino energies. Thus, we recommend to use the Fermi function correction in the range of neutrino energies for which the cross section is below the corresponding EMA value, whereas the EMA could be employed at higher energies, as shown in previ-

ous studies [23, 32].

As a final comment, the QRPA code could be easily extended to calculate ν_μ -induced processes. This was done in Refs. [19, 21] to calculate cross sections using the EMA prescription for the DIF regime of the LSND experiment. The nuclear structure calculations remain the same, while the kinematics changes by changing the electron mass to the muon mass in the variable RMLEP.

-
- [1] A. Aguilar *et al.* [LSND collaboration], Phys. Rev. D **64**, 112007 (2001).
- [2] Y. Fukuda *et al.* [Super-Kamiokande Collaboration], Phys. Rev. Lett. **81**, 1562 (1998); Y. Ashie *et al.* [Super-Kamiokande Collaboration], Phys. Rev. Lett. **93**, 101801 (2004).
- [3] B. Aharmim *et al.* [SNO Collaboration], Phys. Rev. C **59**, 055502 (2005); M. B. Smy *et al.* [Super-Kamiokande Collaboration], Phys. Rev. D **69**, 011104 (2004).
- [4] T. Araki *et al.* [KamLAND Collaboration], Phys. Rev. Lett. **94**, 081801 (2005).
- [5] M. H. Ahn *et al.* [K2K Collaboration], Phys. Rev. Lett. **90**, 041801 (2003).
- [6] G. McLaughlin and G. M. Fuller, Astrop. J. **455**, 202 (1995).
- [7] Y.-Z. Qian and J. Wassweburg, Phys. Rep. **442**, 237 (2007).
- [8] N. Yu. Agafonova *et al.*, Astroparticle Phys. **27**, 254 (2007).
- [9] R. Maschuw *et al.* (KARMEN Collaboration), Prog. Part. Nuc. Phys. **40**, (1998) 183. !; and references therein mentioned.
- [10] B. Armbruster *et al.*, KARMEN collaboration, Phys. Rev. D **65**, 112001 (2002).
- [11] R. C. Allen *et al.*, Phys. Rev. Lett. **64**, 1871 (1990).
- [12] D. A. Krakauer *et al.*, Phys. Rev. C **45**, 2450 (1992).
- [13] C. Athanassopoulos *et al.* [LSND Collaboration], Phys. Rev. C **54**, 2685 (1996); Phys. Rev. Lett. **77**, 3082 (1996).
- [14] C. Athanassopoulos *et al.* [LSND Collaboration], Phys. Rev. C **58**, 2489 (1998); Phys. Rev. Lett. **81**, 1774 (1998).
- [15] Y. Efremenko, Nucl. Phys. **B138**(Proc. Suppl), 343 (2005); F.T. Avignone III and Y.V. Efremenko, J. Phys. G **29**,2615 (2003).
- [16] S.E. Woosley, D. Hartmann, R.D. Hoffman and W.C. Haxton, Astrophys. J. **356**, 272 (1990).
- [17] P. Adamson *et al.* (MINOS Collaboration), Phys. Rev. D **76**, 072005 (2007).
- [18] A.R. Samana, C.A. Bertulani and F. Krmpotić, arXiv:0808.1317v1 [nucl-th].
- [19] F. Krmpotić, A. Mariano and A. Samana, Phys.Lett. **B541**, 298 (2002).
- [20] A. R. Samana and C. A. Bertulani, Phys. Rev. C **78**, 024312 (2008).
- [21] F. Krmpotić, A. Mariano and A. Samana, Phys. Rev. C **71**, 044319 (2005).
- [22] A. Samana, F. Krmpotić, A. Mariano and R. Zukanovich Funchal, Phys. Lett. **B642**, 100 (2006).
- [23] C. Volpe, N. Auerbach, G. Colò, T. Suzuki, N. Van Giai, Phys. Rev. C **62**, 015501 (2000).
- [24] J. Hirsch and F. Krmpotić, Phys. Rev. C **41**, 792 (1990).
- [25] J. Hirsch and F. Krmpotić, Phys. Rev. C **41**, 792 (1990).
- [26] J. Hirsch and F. Krmpotić, Phys. Lett. **B246**, 5 (1990).
- [27] F. Krmpotić, J. Hirsch and H. Dias, Nucl. Phys. **A542**, 85 (1992).
- [28] F. Krmpotić and Shelly Sharma, Nucl. Phys. **A572**, 329 (1994).
- [29] F. Krmpotić, A. Mariano, T.T.S. Kuo, and K. Nakayama, Phys. Lett. **B319**, 393 (1993), and references therein.
- [30] E. Kolbe, K. Langanke and G. Martínez-Pinedo, Phys. Rev. C **60**, 052801(R) (1999).
- [31] R. Lazauskas and C. Volpe, Nucl. Phys. **A792**, 219 (2007).
- [32] N. Paar, D. Vretenar, T. Marketin and P. Ring, Phys. Rev. C **77**, 024608 (2008).
- [33] K. Langanke, G. Martínez-Pinedo, P. von Neumann-Cosel and A. Richter, Phys. Rev. Lett. **93**, 202501 (2004).
- [34] J. Toivanen, E. Kolbe, K. Langanke, G. Martínez-Pinedo, and P. Vogel, Nucl. Phys. **A792**, 219 (2007).
- [35] T.W. Donnelly and W.C. Haxton, Atomic Data and Nuclear Data Tables **23**, 103 (1979); T.W. Donnelly and R. D. Peccei, Phys. Rep. **50**, 1 (1979).
- [36] J. D. Walecka, *Theoretical Nuclear and Subnuclear Physics*, Copyright ©2004 by Imperial College Press and World Scientific Publishing Co. Pte. Ltd.
- [37] T. Kuramoto, M. Fukugita, Y. Kohyama and K. Kubodera, Nucl. Phys. **A512**, 711 (1990).
- [38] R.J. Blin-Stoyle and S.C.K. Nair, Advances in Physics **15**, 493 (1966).
- [39] H. Castillo and F. Krmpotić, Nucl. Phys. **A 469**, 637 (1987).
- [40] H. Behrens and W. Bühring, *Electron Radial Wave Functions and Nuclear Beta Decay* (Clarendon, Oxford, 1982)
- [41] D. J. Rowe, *Nuclear Collective Motion*, Methuen, London, (1970).
- [42] F. Ajzenberg-Selove, Nucl. Phys. **A433**, 1 (1985).
- [43] T. Suzuki *et al.*, Phys. Rev. C **35**, 2212 (1987).
- [44] W.-T. Chou *et al.*, Phys. Rev. C **47**, 163 (1993).
- [45] A. Bohr and B. R. Mottelson, *Nuclear Structure* (Benjamin, New York/Amsterdam, 1969), Vol.I.
- [46] Burton S. Garbow, Kenneth E. Hillstrom and Jorge J. More, Argonne National Laboratory, Minpack Project, March 1980.
- [47] K. Nakayama, A. Pio Galeão and F. Krmpotić, Phys. Lett. **B 114** (1982) 217.
- [48] A. Goswami and M.K. Pal, Nucl. Phys. **35**, (1962) 544.
- [49] D. E. Alburger and A.M. Nathan, Phys. Rev. C **17**, (1978) 280.
- [50] G. H. Miller *et al.*, Phys. Lett. B **41**, 50 (1972).
- [51] E. Kolbe, K. Langanke, G. Martínez-Pinedo and P. Vogel, J. Phys. G **29**, 2569 (2003).
- [52] Subroutine GAULEG, Copr. 1986-92 Numerical Recipes

Software A.

- [53] I. Supek, *Teorijska Fizika-Zagreb*, (1964).
- [54] IMSL Library Reference Manual, Ed. 8, IMSL Inc, , Houston, Texas 77036, 1980. Available in the website: http://ib.cnea.gov.ar/fiscom/Libreria/imsl_old
- [55] K. Ikeda, *Prog. Theor. Phys.* **31**, 434 (1964).
- [56] C. Barbero, F. Krmpotić, and D. Tadić, *Nucl. Phys.* **A628**, 170 (1998); C. Barbero, F. Krmpotić, A. Mari-
ano and D. Tadić, *Nucl. Phys.* **A650**, 485 (1999).
- [57] A.R. Samana, T. Tarutina, F. Krmpotić, M.S. Hussein and T.T.S. Kuo, *Nucl. Phys.* **A791**, 36 (2007).
- [58] J. Engel, *Phys. Rev. C* **57**, 2004 (1998).
- [59] A. Aste and D. Trautmann, *Eur. Phys. J. A* **33**, 11 (2007).